Available online at www.sciencedirect.com
SCIENCE DIRECT®
Journal of Molecular Catalysis A: Chemical 239 (2005) 243–248
JOURNAL OF MOLECULAR CATALYSIS A: CHEMICAL
www.elsevier.com/locate/molcata

In situ XRD, Raman, and TPR studies of CuO/Al_2O_3 catalysts for CO oxidation

Meng-Fei Luo*, Ping Fang, Mai He, Yun-Long Xie

Zhejiang Key Laboratory for Reactive Chemistry on Solid Surfaces, Institute of Physical Chemistry, Zhejiang Normal University, Jinhua 321004, China

Received 26 January 2005; received in revised form 27 April 2005; accepted 14 June 2005
Available online 21 July 2005

Abstract

A series of CuO/Al_2O_3 catalysts for CO oxidation were prepared by impregnation method with different loadings. CuO species and solid–solid interaction in CuO/Al_2O_3 catalysts were characterized by high-temperature in situ XRD, Raman spectroscopy and H_2-TPR techniques. $CuAl_2O_4$ is formed as a result of solid–solid interaction between CuO and Al_2O_3 when the calcination temperature reached 700 °C. Combine with XRD and Raman results, it is found that CuO species is on the surface region of CuO/Al_2O_3 catalysts, while $CuAl_2O_4$ is in the internal layer of CuO. The formation of $CuAl_2O_4$ inhibits CuO diffusing into Al_2O_3 support, which indicates that CuO can stabilize on the surface region of the catalysts at high temperatures. There are three H_2-TPR peaks namely, α_1, α_2 and β, which are attributed to the highly dispersed CuO species, bulk CuO species, and spinel $CuAl_2O_4$, respectively. The activity of CuO/Al_2O_3 catalysts for CO oxidation increased with increasing CuO loading. However, the increase of calcination temperature from 400 to 900 °C resulted in a decrease of the activity in CO oxidation. Combine with H_2-TPR and CO oxidation activity, it is supposed that the catalytic activity is related to both the highly dispersed CuO and bulk CuO.
© 2005 Elsevier B.V. All rights reserved.

Keywords: CuO/Al_2O_3; High-temperature in situ XRD; Raman spectroscopy; Solid–solid interaction; H_2-TPR; CO oxidation

1. Introduction

Copper oxide supported on alumina system is one of the most important catalysts used for several organic reactions, especially widely used in the environmental catalysis area [1,2]. For carbon monoxide oxidation, CuO/Al_2O_3 catalysts even may substitute the noble metals catalysts because of their high catalytic activity [3]. Therefore, CuO/Al_2O_3 catalysts have been widely studied by a variety of instrumental techniques, including X-ray diffraction (XRD), electron spin resonance (ESR), X-ray photoelectron spectroscopy (XPS), thermal analysis (TG-DTA), X-ray absorption fine structure (EXAFS), temperature-programmed reduction (TPR), temperature-programmed desorption (TPD) [4–6], scanning electron micrography (SEM) [7], in situ Fourier transform infrared (FT-IR) [8] spectroscopy et al. However, when the calcination temperature is higher than 700 °C, $CuAl_2O_4$ will be formed by solid–solid interaction between CuO and Al_2O_3 [2,4,9]. Fand et al. [10] reported that conversion of CuO into $CuAl_2O_4$ via solid–solid interaction with Al_2O_3 is normally followed by a decrease in CO oxidation activity simply because CuO exhibited activity higher than that of $CuAl_2O_4$. It is well known that the catalytic activities and thermal stabilization of a great deal of solids can be modified by adding small amount of foreign elements into them [11,12]. Consequently, the addition of small amounts of other cations such as Zn^{2+}, Ca^{2+}, Sr^{2+}, La^{3+}, Ga^{3+}, Cr^{3+}, Sm^{3+}, Ge^{4+}, Zr^{4+}, and Ce^{4+} to the CuO/Al_2O_3 catalysts have been found to influence the chemical interaction between the CuO and Al_2O_3 and exhibit high catalytic performance [3,13,14]. The CuO/Al_2O_3 catalysts also have been prepared in dif-

* Corresponding author. Tel.: +86 579 228 3910; fax: +86 579 228 2595.
E-mail addresses: mengfeiluo@mail.zjnu.net.cn, mengfeiluo@zjnu.cn (M.-F. Luo).

1381-1169/$ – see front matter © 2005 Elsevier B.V. All rights reserved.
doi:10.1016/j.molcata.2005.06.029

ferent methods in order to improve the catalytic properties of CuO/Al_2O_3 catalysts. Chang et al. [7] found the Cu/Al_2O_3 catalysts prepared by electroless planting technique showed a relatively higher acidity than that prepared by other methods. Bond et al. [15] studied the thermal analysis of CuO/Al_2O_3 catalysts precursors using three preparation methods, which were impregnation, ion exchanged, and deposition–precipitation; Miyahara et al. [16] studied the liquid-phase oxidation of benzene to phenol on CuO/Al_2O_3 catalysts prepared by co-precipitation method. Although the oxidation of CO over copper oxide has been studied since 1923, the effect of this solid–solid interaction on the CO oxidation activity needs further investigations.

The aim of the present work is to study the process of the solid–solid interaction between CuO and Al_2O_3 and to investigate the transformation of surface CuO species, the effect of the solid–solid interaction on the CO oxidation activity. The results indicate that the formation of $CuAl_2O_4$ inhibits the reaction of CuO and Al_2O_3, this will give new sight on the study of CuO species and the formation process of $CuAl_2O_4$.

2. Experimental

2.1. Preparation of catalysts

CuO/Al_2O_3 catalysts were prepared by impregnation method with copper nitrate aqueous solution of the desired concentrations. The support was γ-Al_2O_3 with 40–60 meshes and BET surface area is 240 $m^2\,g^{-1}$. The samples were dried at 120 °C and followed calcined at 400, 500, 600, 700, 800, and 900 °C, respectively. The loading amounts of CuO expressed as wt.% CuO in CuO/Al_2O_3 were 1.23, 2.44, 5.88, 11.1, 20.0, 27.3, and 33.3%, respectively. The catalysts were denoted as CuO (*x*%)/Al_2O_3.

CuO was prepared by thermal decomposition of $Cu(NO_3)_2{\cdot}3H_2O$ at 800 °C for 4 h in air. $CuAl_2O_4$ was prepared by mixing stoichiometric amounts of $Cu(NO_3)_2{\cdot}3H_2O$ and $Al(NO_3)_3{\cdot}9H_2O$ in distilled water and heating at 120 °C overnight. The resultant mixture was finely ground and subsequently calcined at 800 °C for 4 h.

2.2. XRD analysis of crystal phase

X-ray diffraction (XRD) patterns were collected on a PHILIPS PW 3040/60 powder diffractometer using Cu Kα radiation. The working voltage of the instrument was 40 kV and the current was 40 mA. The intensity data were collected at 25 °C in a 2θ range from 20° to 75° with a scan rate of 0.1° s^{-1}. The high-temperature experiments were carried out using an X-ray reactor chamber XRK-900 Anton Paar, in which the scan rate was 0.1° s^{-1} and the XRD patterns were recorded at the reductive atmosphere. The reductive gas contained 5% H_2 and 95% N_2.

2.3. Laser Raman spectra

Room-temperature Raman were excited at 632.8 nm using a He–Ne laser. Spectra were obtained with a Renishaw RM1000 confocal microscope. The resolution is ±1 cm^{-1}.

UV–vis absorption spectra were recorded on a JASCO V-550 spectrophotometer equipped with an integrating sphere.

2.4. H_2-TPR

The reduction properties of CuO/Al_2O_3 catalysts were measured by means of temperature-programmed reduction (TPR) techniques. A 10 mg sample was placed in a quartz reactor which was connected to a conventional TPR apparatus, The reactor was heated form room temperature to 900 °C at a heating rate of 20 °C min^{-1} and the amount of H_2 uptake during the reduction was measured by thermal conductivity detector (TCD).

2.5. Catalytic activity of CO oxidation

Catalytic activity measurements were carried out in a fixed bed reactor (6 mm i.d.) using 150 mg catalyst. The total flow rate of the feed gas was 80 ml min^{-1}. The catalysts were directly exposed to reaction gas as the reactor temperature stabilized at the reaction temperature without any pretreatment. For CO oxidation, the gas consisted of 2.4% CO and 1.2% O_2 in N_2 with a total flow rate 80 ml (NTP) min^{-1}. The analysis of the CO_2 concentration in the reactor effluent was performed by means of a GC (13× molecular sieve and Propark Q) equipped with a thermal conductivity detector (TCD).

3. Results and discussion

3.1. Phase analysis of catalysts

The XRD patterns of CuO (33.3%)/Al_2O_3 catalysts calcined at different temperatures are shown in Fig. 1. The crystalline phase were identified in comparison with ICDD files. (CuO, PDF No. 80-1268; $CuAl_2O_4$, PDF No. 78-1605.) The diffraction peaks of CuO gradually decrease with increasing calcination temperature. On the other hand, $CuAl_2O_4$ diffraction peaks appear at 700 °C, and the intensity of $CuAl_2O_4$ diffraction peaks increases with increasing calcination temperature from 700 to 800 °C, but further increasing the calcination temperature, the intensity of the diffraction peaks at 900 °C is closed to that at 800 °C. This indicates that $CuAl_2O_4$ layer formed by solid–solid interaction between CuO and Al_2O_3 inhibits CuO diffusing into Al_2O_3 support.

Fig. 2 shows the XRD patterns of CuO (*x*%)/Al_2O_3 catalysts calcined at 800 °C. For Al_2O_3 support calcined at 800 °C, weak diffraction peaks of γ-Al_2O_3 and θ-Al_2O_3 are observed. There are no visible diffraction lines due to CuO at low CuO loading (<5.88%). This indicates CuO species

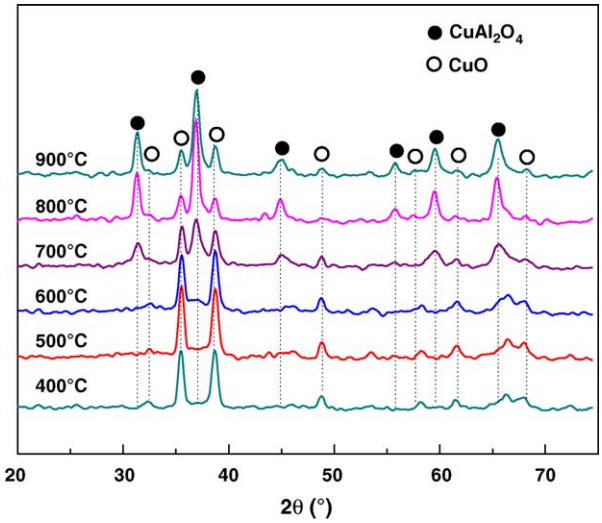

Fig. 1. XRD patterns of CuO (33.3%)/Al_2O_3 catalysts calcined at different temperatures.

on the alumina surface exist as highly dispersed species. As the CuO loading increases to 5.88%, the diffraction peaks of $CuAl_2O_4$ become apparented. However, the CuO phase is not detected until CuO loading is higher than 11.1%. The intensity of $CuAl_2O_4$ diffraction peaks increases with increasing CuO loading from 5.88 to 20.0%. After CuO loading is higher than 20.0%, the intensity of $CuAl_2O_4$ diffraction peak is closed to that of 20.0%. This indicates that a part of CuO changes into $CuAl_2O_4$ via solid–solid interaction with Al_2O_3 [10]. By the time that a large amount of $CuAl_2O_4$ has formed, the $CuAl_2O_4$ layer inhibits CuO diffusing into Al_2O_3 support.

3.2. Raman spectra analysis of catalysts

Fig. 3 shows the laser Raman spectra of CuO (33.3%)/Al_2O_3 catalysts calcined at different temperatures. For CuO (33.3%)/Al_2O_3 catalysts calcined at different temperatures,

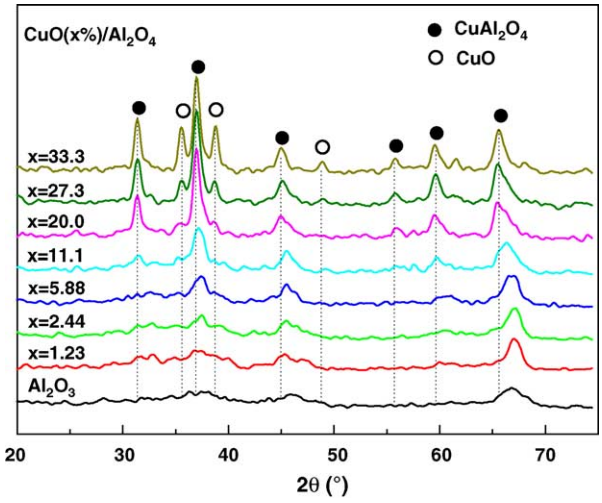

Fig. 2. XRD patterns of CuO (*x*%)/Al_2O_3 catalysts calcined at 800 °C.

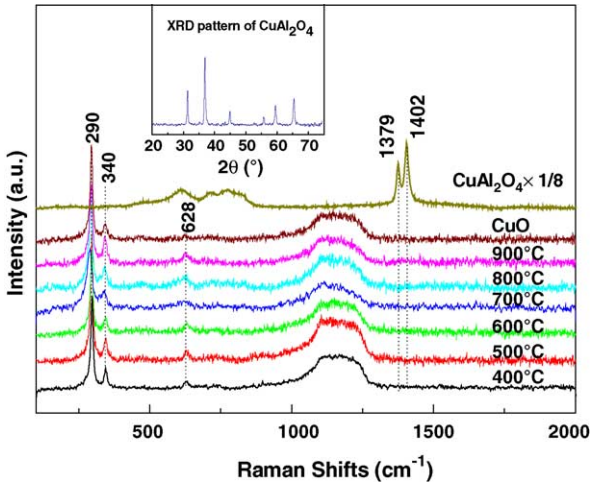

Fig. 3. Laser Raman spectra of CuO (33.3%)/Al_2O_3 catalysts calcined at different temperatures.

three bands at 290, 340, and 628 cm^{-1} are observed. These bands are attributed to the bulk CuO [17,18]. For $CuAl_2O_4$ sample, two bands at 1379 and 1402 cm^{-1} are observed. Although XRD can detect both bulk CuO and spinel $CuAl_2O_4$ in CuO (33.3%)/Al_2O_3 catalysts, in Raman spectra only bulk CuO is observed.

Fig. 4 shows the laser Raman spectra of CuO/Al_2O_3 catalysts calcined at 800 °C with different CuO loadings. For Al_2O_3 calcined at 800 °C there are two obvious bands at 1179 and 1230 cm^{-1} are observed, and the relatively weak bands at 1379 and 1402 cm^{-1} also can be observed. With increasing CuO loading from 1.23 to 11.1%, the intensity of bands at 1179 and 1230 cm^{-1} diminishes till disappears, while the intensity of bands at 1379 and 1402 cm^{-1} increases obviously. When CuO loading is higher than 20.0%, the bands at 1379 and 1402 cm^{-1} disappear; meanwhile, the Raman bands of bulk CuO appear. Under the excitation of 632.8 nm, the two strongest bands at Raman shifts of 1379 and 1402 cm^{-1} are

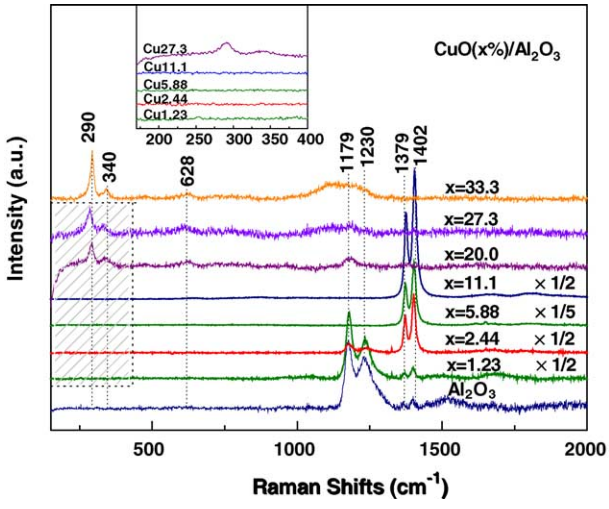

Fig. 4. Laser Raman spectra of CuO (x%)/Al_2O_3 catalysts calcined at 800 °C.

closed to the strong emission centered to band at 693.3 nm and 694.4 nm of the Cr^{3+} and Fe^{3+} fluorescence band in a spinel or α-Al_2O_3 environment [19–22]. Meanwhile, the bands at 1179 and 1230 cm^{-1} are closed to emission bands centered at 683.8 and 686.2 nm of the Cr^{3+} fluorescence bands in θ-Al_2O_3 environment [19]. As α-Al_2O_3 is not observed in XRD patterns, in addition, α-Al_2O_3 only forms at higher than 1100 °C. As we know, $CuAl_2O_4$ has the same spinel structure as α-Al_2O_3 [20]. Therefore, the strong bands at 1379 and 1402 cm^{-1} are attributed to the emission bands at 693.3 and 694.4 nm of the impurity Cr^{3+} and Fe^{3+} fluorescence in $CuAl_2O_4$ environment.

Generally speaking, Raman spectra can record the Raman bands of surface region and the bulk of the sample at the same time, but when the sample has a strong absorption on the Raman laser, then the Raman spectra mainly afford the information at the surface region [23]. Fig. 5 shows the UV–vis diffuse reflectance spectra of CuO (33.3%)/Al_2O_3 catalyst calcined at 800 °C. There is a broad absorption band from 220 to 700 nm and the electronic absorption of CuO (33.3%)/Al_2O_3 is very strong. The laser radiation used as the excitation in this work was at 632.8 nm, which is in the electronic adsorption area of the sample. So the catalyst can adsorb most of the Raman laser that enter into the bulk of the sample, then the Raman spectra can separate the information of surface region from the bulk of the sample [23]. In another words, the Raman spectroscopy is found to be more sensitive at surface region while XRD supply the information mainly from the bulk. As we know that the results from XRD reveal the information of the surface and bulk totally. At high CuO loading only CuO is observed in Raman spectra. This leads us to conclude that $CuAl_2O_4$ is in the intermediate between surface CuO and Al_2O_3 support. With increasing the yield of $CuAl_2O_4$ at high temperature, in other words, to enhance the thickness of $CuAl_2O_4$ layer, CuO on the surface region becomes more difficult to diffuse into Al_2O_3 support, then the residual CuO can stabilize on the surface region. Although in low CuO loadings we cannot see obvious XRD diffraction peaks or Raman bands that refer to CuO, it does not mean that there are no CuO exist, as the highly dispersed CuO cannot give the corresponding viewable information.

3.3. H_2-TPR of catalysts

Fig. 6 shows the H_2-TPR profiles of CuO (33.3%)/Al_2O_3 catalysts calcined at different temperatures. It can be seen there are three H_2-TPR peaks, namely, α_1 (230–255 °C), α_2 (275–300 °C), and β (450–490 °C). With increasing calcination temperature the intensity of peak α_1 increases slowly and the position of that shifts to lower temperature. However, the intensity of peak α_1 reaches the maximum for the catalyst calcined at 600 °C, and the position of that shifts to the lowest temperature for the catalysts calcined at 700 °C. The intensity of peak α_2 monotonously decreases with increasing calcination temperature. After the catalysts calcined at 700 °C, the intensity of peak α_2 is closed to half of that at 600 °C. In addition, peak β appears for the catalysts calcined at 700 °C and above.

In order to reveal the attribution of TPR peaks, in situ XRD patterns is measured under the flowing mixed gas whose component is the same as the H_2-TPR gas. Fig. 7 is in situ XRD patterns of CuO (33.3%)/Al_2O_3 catalyst calcined at 800 °C. From Fig. 7, it can be seen that the intensity of diffraction peaks at 250 °C is similar to that at 25 °C. Diffraction peaks of CuO disappear after temperature reaches 300 °C while crystalline Cu is observed. The intensity of diffraction peaks of $CuAl_2O_4$ gradually diminishes from 400 to 800 °C. Combined with Fig. 6, that TPR peak α_1 is attributed to reduction of highly dispersed CuO species, peak α_2 is contributed to the reduction of bulk CuO species; peak β is attributed to reduction of $CuAl_2O_4$.

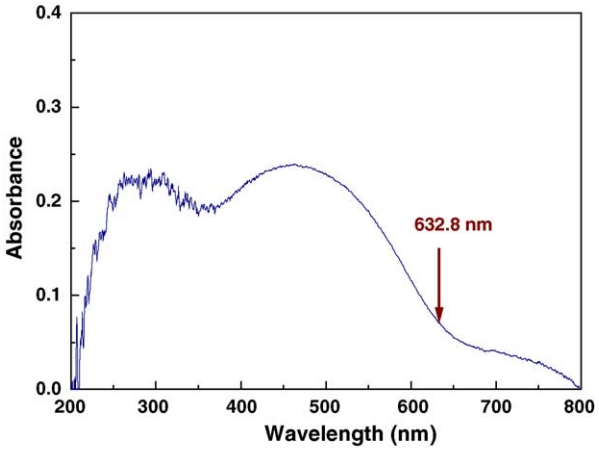

Fig. 5. UV–vis diffuse reflectance spectra of CuO (33.3%)/Al_2O_3 catalyst calcined at 800 °C.

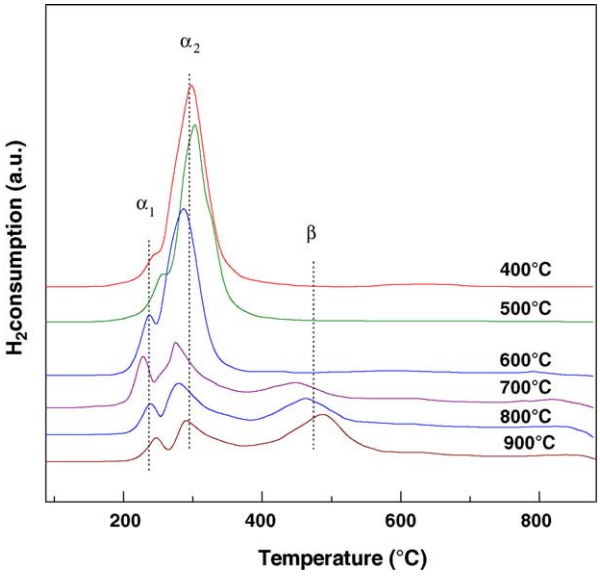

Fig. 6. H_2-TPR profiles of CuO (33.3%)/Al_2O_3 catalysts calcined at different temperatures.

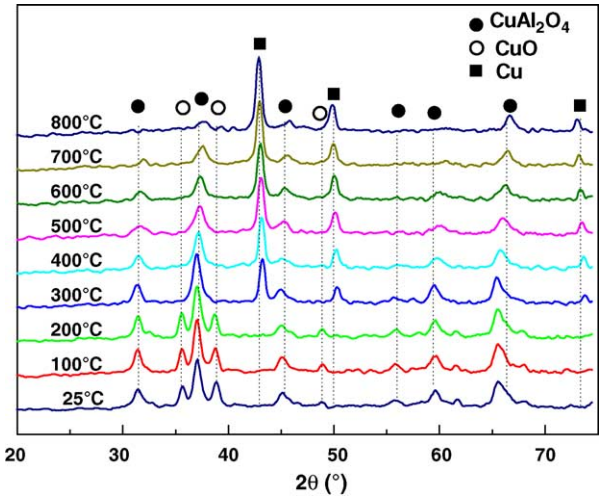

Fig. 7. In situ XRD patterns under the flowing mixture gas of H_2 (5%)–N_2 (95%) for CuO (33.3%)/Al_2O_3 catalyst calcined at 800 °C.

The H_2-TPR profiles of CuO/Al_2O_3 catalysts calcined at 800 °C with different CuO loadings are showed in Fig. 8. Compared with Fig. 6, it implies that peaks α_1, α_2 and β are attributed to the reduction of the highly dispersed CuO, bulk CuO [24,25] and spinel $CuAl_2O_4$ [26], respectively. With increasing the CuO loading the intensity of peak α_1 increases and shifts to lower temperature, meanwhile, a new and weak peak β appears at relatively high temperature (about 470 °C). Peak β obviously increases after the CuO loading increases to 20.0%, at the same time the peak α_2 is observed. Further increasing CuO loading, the changes of peak α_1 and β are not evidently, but peaks α_2 has increased obviously. This suggests that both the highly dispersed CuO and $CuAl_2O_4$ exist at low CuO loading, contrarily, bulk CuO appears merely at high CuO loading (>5.88%). From the TPR results, it indicates that there are highly dispersed CuO on the surface at low CuO loading. These highly dispersed CuO (small CuO dust) are not detectable by XRD and Raman spectroscopy.

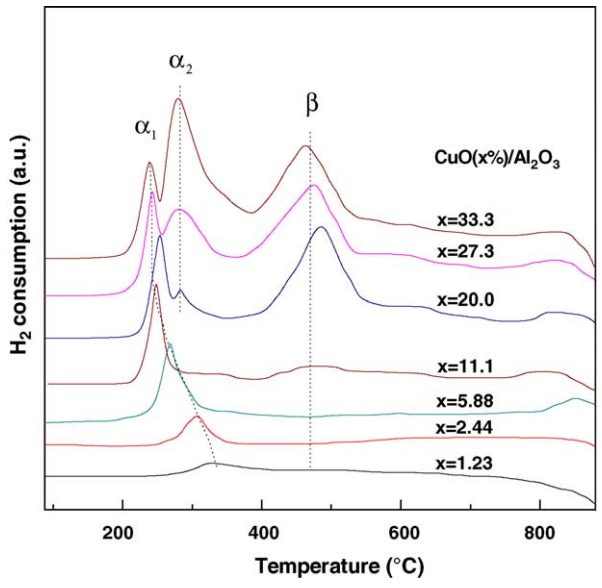

Fig. 8. H_2-TPR profiles of CuO (x%)/Al_2O_3 catalysts calcined at 800 °C.

3.4. The catalytic activity for CO oxidation

Fig. 9 shows the activity of CuO (33.3%)/Al_2O_3 catalysts calcined at different temperatures for CO oxidation. The activity of $CuAl_2O_4$ alone is also showed for comparing. As the calcination temperature increasing from 400 to 600 °C, the catalytic activity decreases gradually. However, the catalytic activities reduce obviously when the calcination temperature exceeds 700 °C, and the activity of $CuAl_2O_4$ is the lowest. Combined with H_2-TPR (Fig. 6), due to the intensity of peak α_1 does not change evidently, but the intensity of peak α_2 for the catalysts calcined at 600, 700, and 800 °C is closed to half of that at 400, 500, and 600 °C. This shows that the CO oxidation activity of CuO (33.3%)/Al_2O_3 catalysts is chiefly related to the bulk CuO.

Fig. 10 shows the activity of CuO/Al_2O_3 catalysts calcined at 800 °C with various CuO loadings for CO oxidation. The catalytic activity of CuO/Al_2O_3 catalysts enhances with increasing the CuO loading. However, the activity increases slowly when the CuO loading exceeds 5.88%. This indicates that conversion of CuO into $CuAl_2O_4$ via solid–solid interaction with Al_2O_3 is normally followed by a decrease in CO oxidation activity simply because CuO exhibited activity higher than that of $CuAl_2O_4$ [10]. Combined with TPR results in Fig. 8, as the CuO loading exceeds 5.88%, the intensity of peak α_1 increases slowly and the position of that shifts to lower temperature, while peak α_2 appears and increases quickly. This suggests that the CO oxidation activity of CuO/Al_2O_3 catalysts with different loading is mainly related to the highly dispersed CuO species. Connect with Figs. 9 and 10, it is supposed that the CO oxi-

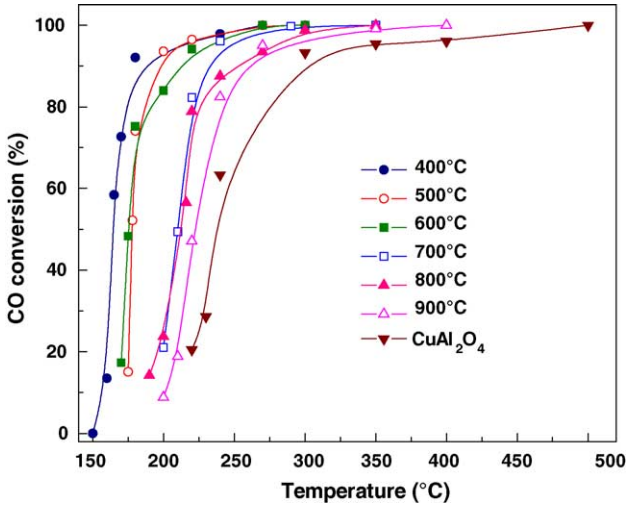

Fig. 9. Activity of CuO (33.3%)/Al_2O_3 catalysts calcined at different temperatures for CO oxidation.

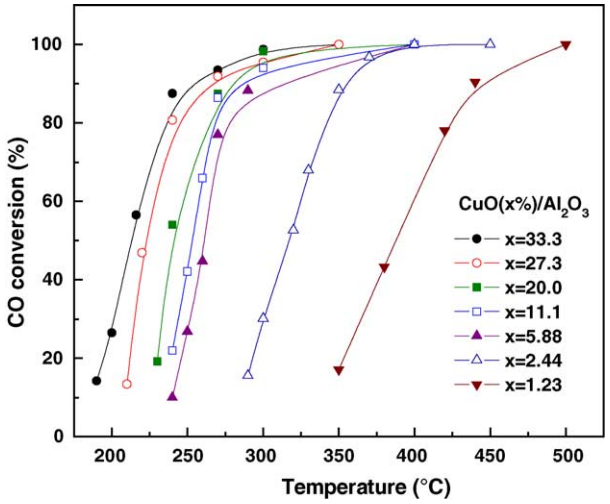

Fig. 10. Activity of CuO (x%)/Al_2O_3 catalysts calcined at 800 °C for CO oxidation.

dation activities are related to both the highly dispersed CuO species and the bulk CuO species. The highly dispersed CuO has stronger effect on the catalytic activities than the bulk CuO. In totally, the CO oxidation activity of CuO/Al_2O_3 catalysts calcined at different temperatures is related to the highly dispersed CuO species, meanwhile, the catalysts with different loadings show better matching with the bulk CuO.

4. Conclusions

Crystalline $CuAl_2O_4$ has formed by solid–solid interaction in CuO/Al_2O_3 catalysts after calcined at 700 °C and above. As the yield of $CuAl_2O_4$ increases, the CuO in the surface region becomes more difficult to diffuse into the support then can stabilize on the surface of the catalysts. There are three H_2-TPR peaks for CuO/Al_2O_3 catalysts, namely, α_1, α_2, and β. Combined with in situ XRD, the three peaks were attributed to the highly dispersed CuO species, bulk CuO species and spinel $CuAl_2O_4$, respectively. The results of CO oxidation activity indicate that the catalytic activities are related to both the highly dispersed CuO species and bulk CuO species.

Acknowledgment

The support by the Natural Science Foundation of Zhejiang Province (Grant M203147) is acknowledged.

References

[1] T.W. Kim, M.W. Song, H.L. Koh, K.L. Kim, Appl. Catal. A 210 (2001) 35.
[2] W.M. Shaheen, Thermochim. Acta 385 (2002) 105.
[3] N.A.M. Deraz, Colloid Surf. A 207 (2002) 197.
[4] R.M. Friedman, J.J. Freeman, F.W. Lytle, J. Catal. 55 (1978) 10.
[5] B.R. Strohmeier, D.E. Leyden, R.S. Field, D.M. Hercules, J. Catal. 94 (1985) 514.
[6] W.R.A.M. Robinson, J.C. Mol, Appl. Catal. 44 (1988) 165.
[7] H.F. Chang, M.A. Saleque, W.S. Hsu, W.H. Lin, J. Mol. Catal. A 109 (1996) 249.
[8] J.W. Bijsterbosch, F. Kapteijn, J.A. Moulijn, J. Mol. Catal. 74 (1992) 193.
[9] J.M. Dumas, C. Geron, A. Kribii, J. Barbier, Appl. Catal. 47 (1989) 9.
[10] S.N. Fand, P.Y. Lin, Y.L. Fu, J. Mol. Catal. 8 (1994) 86.
[11] G.A. El-Shobaky, A.M. Turky, Adv. Sci. Technol. 17 (1999) 575.
[12] S. Imamura, M. Shono, N. Okamoto, A. Hamada, S. Ishida, Appl. Catal. A 142 (1996) 279.
[13] N.R.E. Radwan, G.A. Fagal, G.A. El-Shobaky, Colloid Surf. A 178 (2001) 277.
[14] X.Y. Jiang, R.X. Zhou, P. Pan, B. Zhu, X.X. Yuan, X.M. Zheng, Appl. Catal. A 150 (1997) 131.
[15] G.C. Bond, S.N. Namijo, J.S. Wakeman, J. Mol. Catal. 64 (1991) 305.
[16] T. Miyahara, H. Kanzaki, R. Hamada, S. Kuroiwa, S. Nishiyama, S. Tsuruya, J. Mol. Catal. A 176 (2001) 141.
[17] J.F. Xu, W. Ji, Z.X. Shen, W.S. Li, S.H. Tang, X.R. Ye, D.Z. Jia, X.Q. Xin, J. Raman Spectrosc. 30 (1999) 413.
[18] P.O. Larsson, A. Andersson, J. Catal. 179 (1998) 72.
[19] J. Kákoš, L. Bača, P. Veis, L. Pach, J. Sol–Gel Sci. Technol. 21 (2001) 167.
[20] A. Aminzadeh, Appl. Spectrosc. 51 (1997) 817.
[21] M. Kadlečíková, J. Breza, M. Veselý, I. Červeň, Microelectron. J. 34 (2003) 95.
[22] S.V. Bulyarskii, A.E. Kozhevin, S.N. Mikov, V.V. Prikhodko, Phys. State Solid A 180 (2000) 555.
[23] C. Li, M.J. Li, J. Raman Spectrosc. 33 (2002) 301.
[24] M.F. Luo, Y.J. Zhong, X.X. Yuan, X.M. Zheng, Appl. Catal. A 162 (1997) 121.
[25] M.F. Luo, X.M. Zheng, Acta Chem. Scand. 52 (1998) 1183.
[26] S. Sato, M. Iijima, T. Nakayama, T. Sodesawa, F. Nozaki, J. Catal. 169 (1997) 447.